

Hg²⁺-Reactive Double Hydrophilic Block Copolymer Assemblies as Novel Multifunctional Fluorescent Probes with Improved Performance

Jinming Hu, Changhua Li, and Shiyong Liu*

CAS Key Laboratory of Soft Matter Chemistry, Department of Polymer Science and Engineering, Hefei National Laboratory for Physical Sciences at the Microscale, University of Science and Technology of China, Hefei, Anhui 230026, China

Received July 6, 2009. Revised Manuscript Received August 24, 2009

We report on novel type of responsive double hydrophilic block copolymer (DHBC)-based multifunctional chemosensors to Hg²⁺ ions, pH, and temperatures and investigate the effects of thermo-induced micellization on the detection sensitivity. Well-defined DHBCs bearing rhodamine B-based Hg²⁺-reactive moieties (RhBHA) in the thermo-responsive block, poly(ethylene oxide)-*b*-poly(*N*-isopropylacrylamide-*co*-RhBHA) (PEO-*b*-P(NIPAM-*co*-RhBHA)), were synthesized via reversible addition-fragmentation chain transfer (RAFT) polymerization. Nonfluorescent RhBHA moieties are subjected to selective ring-opening reaction upon addition of Hg²⁺ ions or lowering solution pH, producing highly fluorescent acyclic species. Thus, at room temperature PEO-*b*-P(NIPAM-*co*-RhBHA) DHBCs can serve as water-soluble multifunctional and efficient fluorescent chemosensors to Hg²⁺ ions and pH. Upon heating above the lower critical solution temperature (~36 °C) of the PNIPAM block, they self-assemble into micelles possessing P(NIPAM-*co*-RhBHA) cores and well-solvated PEO coronas, which were fully characterized by dynamic and static laser light scattering. It was found that the detection sensitivity to Hg²⁺ ions and pH could be dramatically improved at elevated temperatures due to fluorescence enhancement of RhBHA residues in the acyclic form, which were embedded within hydrophobic cores of thermo-induced micellar aggregates. This work represents a proof-of-concept example of responsive DHBC-based multifunctional fluorescent chemosensors for the highly efficient detection of Hg²⁺ ions, pH, and temperatures with tunable detection sensitivity. Compared to reaction-based small molecule Hg²⁺ probes in previous literature reports, the integration of stimuli-responsive block copolymers with well-developed small molecule-based selective sensing moieties in the current study are expected to exhibit preferred advantages including enhanced detection sensitivity, water dispersibility, biocompatibility, facile incorporation into devices, and the ability of further functionalization for targeted imaging and detection.

Introduction

Mercury pollutant poses a huge threat to human beings and our environment due to its bioaccumulation, long residence, and permanent damage in central nervous and endocrine systems.¹ Thus, highly sensitive and selective detection and imaging of Hg²⁺ ions in tissues and organisms is quite crucial. Previously, a variety of fluorescent and colorimetric Hg²⁺ chemosensors

based on small molecules,^{2–17} conjugated polymers,^{18–20} nanoparticles,^{21–26} and biomolecules^{23,27–33} were reported. Current efforts in this field have focused on the development

*To whom correspondence should be addressed. E-mail: sliu@ustc.edu.cn.
(1) Clarkson, T. W.; Magos, L.; Myers, G. J. *N. Engl. J. Med.* **2003**, *349*, 1731–1737.

(2) Kim, H. N.; Lee, M. H.; Kim, H. J.; Kim, J. S.; Yoon, J. *Chem. Soc. Rev.* **2008**, *37*, 1465–1472.

(3) Nolan, E. M.; Lippard, S. J. *Chem. Rev.* **2008**, *108*, 3443–3480.

(4) Nolan, E. M.; Lippard, S. J. *J. Am. Chem. Soc.* **2003**, *125*, 14270–14271.

(5) Nolan, E. M.; Lippard, S. J. *J. Am. Chem. Soc.* **2007**, *129*, 5910–5918.

(6) Descalzo, A. B.; Martinez-Manez, R.; Radeaglia, R.; Rurack, K.; Soto, J. *J. Am. Chem. Soc.* **2003**, *125*, 3418–3419.

(7) Coskun, A.; Akkaya, E. U. *J. Am. Chem. Soc.* **2006**, *128*, 14474–14475.

(8) Ono, A.; Togashi, H. *Angew. Chem., Int. Ed.* **2004**, *43*, 4300–4302.

(9) Wu, D.; Descalzo, A. B.; Weik, F.; Emmerling, F.; Shen, Z.; You, X. Z.; Rurack, K. *Angew. Chem., Int. Ed.* **2008**, *47*, 193–197.

(10) Wegner, S. V.; Okesli, A.; Chen, P.; He, C. A. *J. Am. Chem. Soc.* **2007**, *129*, 3474–.

(11) Brummer, O.; La Clair, J. J.; Janda, K. D. *Org. Lett.* **1999**, *1*, 415–418.

(12) Caballero, A.; Martinez, R.; Lloveras, V.; Ratera, I.; Vidal-Gancedo, J.; Wurst, K.; Tarraga, A.; Molina, P.; Veciana, J. *J. Am. Chem. Soc.* **2005**, *127*, 15666–15667.

(13) Chae, M. Y.; Czarnik, A. W. *J. Am. Chem. Soc.* **1992**, *114*, 9704–9705.

(14) Coronado, E.; Galan-Mascaros, J. R.; Marti-Gastaldo, C.; Palomares, E.; Durrant, J. R.; Vilar, R.; Gratzel, M.; Nazeeruddin, M. K. *J. Am. Chem. Soc.* **2005**, *127*, 12351–12356.

(15) Guo, X. F.; Qian, X. H.; Jia, L. H. *J. Am. Chem. Soc.* **2004**, *126*, 2272–2273.

(16) Ros-Lis, J. V.; Marcos, M. D.; Martinez-Manez, R.; Rurack, K.; Soto, J. *Angew. Chem., Int. Ed.* **2005**, *44*, 4405–4407.

(17) Sancenon, F.; Martinez-Manez, R.; Soto, J. *Chem. Commun.* **2001**, 2262–2263.

(18) Thomas, S. W.; Joly, G. D.; Swager, T. M. *Chem. Rev.* **2007**, *107*, 1339–1386.

(19) Fan, L. J.; Zhang, Y.; Jones, W. E. *Macromolecules* **2005**, *38*, 2844–2849.

(20) Liu, X. F.; Tang, Y. L.; Wang, L. H.; Zhang, J.; Song, S. P.; Fan, C. H.; Wang, S. *Adv. Mater.* **2007**, *19*, 1662–1662.

(21) Darbha, G. K.; Ray, A.; Ray, P. C. *ACS Nano* **2007**, *1*, 208–214.

(22) Huang, C. C.; Chang, H. T. *Anal. Chem.* **2006**, *78*, 8332–8338.

(23) Lee, J. S.; Mirkin, C. A. *Anal. Chem.* **2008**, *80*, 6805–6808.

(24) Rex, M.; Hernandez, F. E.; Campiglia, A. D. *Anal. Chem.* **2006**, *78*, 445–451.

(25) Huang, C. C.; Yang, Z.; Lee, K. H.; Chang, H. T. *Angew. Chem., Int. Ed.* **2007**, *46*, 6824–6828.

(26) Lee, S. J.; Lee, J. E.; Seo, J.; Jeong, I. Y.; Lee, S. S.; Jung, J. H. *Adv. Funct. Mater.* **2007**, *17*, 3441–3446.

(27) Ivask, A.; Hakkila, K.; Virta, M. *Anal. Chem.* **2001**, *73*, 5168–5171.

(28) Kim, I. B.; Bunz, U. H. F. *J. Am. Chem. Soc.* **2006**, *128*, 2818–2819.

(29) Lee, J. S.; Han, M. S.; Mirkin, C. A. *Angew. Chem., Int. Ed.* **2007**, *46*, 4093–4096.

(30) Matsushita, M.; Meijler, M. M.; Wirsching, P.; Lerner, R. A.; Janda, K. D. *Org. Lett.* **2005**, *7*, 4943–4946.

(31) Miyake, Y.; Togashi, H.; Tashiro, M.; Yamaguchi, H.; Oda, S.; Kudo, M.; Tanaka, Y.; Kondo, Y.; Sawa, R.; Fujimoto, T.; Machinami, T.; Ono, A. *J. Am. Chem. Soc.* **2006**, *128*, 2172–2173.

(32) Ou, S. J.; Lin, Z. H.; Duan, C. Y.; Zhang, H. T.; Bai, Z. P. *Chem. Commun.* **2006**, 4392–4394.

(33) Zhu, X. J.; Fu, S. T.; Wong, W. K.; Guo, H. P.; Wong, W. Y. *Angew. Chem., Int. Ed.* **2006**, *45*, 3150–3154.

of ratiometric,^{34–36} water-soluble,^{37–40} and cell-permeable Hg²⁺ sensing ensembles.^{41,42} As originated by the work of Tae et al.^{43–45} in 2005, leuco-rhodamine derivative-based mercury sensors have aroused a great deal of interest, which take advantage of the highly selective Hg²⁺-mediated ring-opening reaction of initially nonfluorescent spirolactam compounds. However, these rhodamine-based chemosensors typically exhibit poor water solubility, and this partially limits their potential applications in biological systems.

Recently, the concept of self-organization has also been introduced to the field of ion-selective chemosensors to realize functional cooperativity and adaptability, using surfactant micelles and functionalized silica nanoparticles as the sensing matrix.^{46–54} To the best of our knowledge, self-assembled block copolymer aggregates have been less explored as a platform for designing novel type of sensing ensembles. It has been well-established that stimuli-responsive double hydrophilic block copolymers (DHBCs) can self-assemble into one or more types of aggregates in aqueous solution under proper external stimuli such as pH and temperature, the changes of which are typically observed in disease regions and can be conveniently manipulated in living organisms.^{55–62} Therefore, we speculate that the incorporation of ion-selective sensing moieties into DHBCs should enable the development of multifunctional (pH, temperature, ions, etc.) chemosensors with combined advantages including water dispersibility, biocompatibility, facile integration into devices, and the ability of further functionalization for targeting purposes.^{55,58}

Most importantly, hydrophobic domains in self-assembled DHBC aggregates can help achieve signal amplification of fluorescent reporter moiety in sensing ensembles, which can further enhance the detection sensitivity.^{63–67}

It has been well-established that nonfluorescent rhodamine urea derivative in the spirolactam form, serving as a fluorescence “turn-on” moiety, can be selectively converted into the fluorescent ring-opened amide form in the presence of Hg²⁺ ions or in acidic media (Scheme 1a).^{2,43–45,63} In this work, we report on the synthesis of water-soluble DHBCs bearing rhodamine B (RhB)-based Hg²⁺-sensing moieties in the thermo-sensitive block, poly(ethylene oxide)-*b*-poly(*N*-isopropylacrylamide-*co*-RhBHA) (PEO-*b*-P(NIPAM-*co*-RhBHA)), which can serve as multifunctional sensors to pH, temperature, and Hg²⁺ ions (Scheme 1b). Moreover, thermo-induced aggregation of DHBCs can further improve detection sensitivities of pH and Hg²⁺ ions due to the embedding of fluorescent reporters within hydrophobic cores.

Experimental Section

Materials. Poly(ethylene oxide) monomethyl ether (PEO₁₁₃-OH, $M_{n,GPC} = 5.0$ kDa, $M_w/M_n = 1.06$ (PEO standards); mean degree of polymerization, DP, is 113) was purchased from Aldrich and used as received. *N*-Isopropylacrylamide (NIPAM, 97%, Tokyo Kasei Kogyo) was recrystallized twice from a mixture of *n*-hexane and benzene (v/v = 2:1) prior to use. Rhodamine B (RhB, Acros), *N,N'*-dicyclohexylcarbodiimide (DCC), 4-(dimethylamino)pyridine (DMAP), potassium thiocyanate (KSCN), hydrazine hydrate, and all other reagents (Sinopharm Chemical Reagent Co.) were used as received. Acryloyl chloride (Sinopharm Chemical Reagent Co.) was distilled prior to use. 2,2'-Azobisisobutyronitrile (AIBN) was recrystallized from 95% ethanol. Dichloromethane (CH₂Cl₂) and acetonitrile (MeCN) were dried over CaH₂ and distilled just prior to use. Toluene was distilled over sodium shavings and benzophenone immediately before use. Perchlorate salts (K⁺, Na⁺, Li⁺, Co²⁺, Cd²⁺, Pb²⁺, Zn²⁺, Fe²⁺, Fe³⁺, Ca²⁺, Ag⁺, Cu²⁺, and Hg²⁺) were used for experiments. Water was deionized with a Milli-Q SP reagent water system (Millipore) to a specific resistivity of 18.4 MΩ cm. 3-(Benzylthiocarbonothioylthio)propanoic acid (BTPA) and Rhodamine B hydrazide were synthesized according to literature procedures.^{68,69}

Sample Synthesis. Synthetic schemes employed for the preparation of RhB-based Hg²⁺-sensing monomer, RhBHA, PEO-based macroRAFT agent, and PEO-*b*-P(NIPAM-*co*-RhBHA) DHBCs are shown in Schemes S1 and S2 in the Supporting Information.

Synthesis of Acryloyl Isothiocyanate. Anhydrous potassium thiocyanate (9.72 g, 0.1 mol) and poly(ethylene glycol) monomethyl ether (PEG₆-OH, $M_n = 300$; 0.9 g, 3.0 mmol) were dissolved in dry CH₂Cl₂ (100 mL) and cooled to 0 °C in an ice–water bath. Acryloyl chloride (9.05 g, 0.1 mol) in dry CH₂Cl₂ (20 mL) was then added dropwise over 2 h. The reaction mixture was stirred at room temperature for 2 h and then quickly filtered over a Buchner funnel. After removing all the solvents, acryloyl isothiocyanate was obtained as a colorless liquid by vacuum distillation (8.4 g, yield: 74%). ¹H NMR (CDCl₃, δ, ppm, TMS): 6.52

(34) Ben Othman, A.; Lee, J. W.; Wu, J. S.; Kim, J. S.; Abidi, R.; Thuery, P.; Strub, J. M.; Van Dorselaer, A.; Vicens, J. *J. Org. Chem.* **2007**, *72*, 7634–7640.

(35) Liu, B.; Tian, H. *Chem. Commun.* **2005**, 3156–3158.

(36) Zhang, X. L.; Xiao, Y.; Qian, X. H. *Angew. Chem., Int. Ed.* **2008**, *47*, 8025–8029.

(37) Czarnik, A. W. *Acc. Chem. Res.* **1994**, *27*, 302–308.

(38) Dickerson, T. J.; Reed, N. N.; LaClair, J. J.; Janda, K. D. *J. Am. Chem. Soc.* **2004**, *126*, 16582–16586.

(39) Nolan, E. M.; Racine, M. E.; Lippard, S. J. *Inorg. Chem.* **2006**, *45*, 2742–2749.

(40) Ros-Lis, J. V.; Martinez-Manez, R.; Rurack, K.; Sancenon, F.; Soto, J.; Spieles, M. *Inorg. Chem.* **2004**, *43*, 5183–5185.

(41) Yoon, S.; Albers, A. E.; Wong, A. P.; Chang, C. J. *J. Am. Chem. Soc.* **2005**, *127*, 16030–16031.

(42) Yoon, S.; Miller, E. W.; He, Q.; Do, P. H.; Chang, C. J. *Angew. Chem., Int. Ed.* **2007**, *46*, 6658–6661.

(43) Yang, Y. K.; Yook, K. J.; Tae, J. *J. Am. Chem. Soc.* **2005**, *127*, 16760–16761.

(44) Ko, S. K.; Yang, Y. K.; Tae, J.; Shin, I. *J. Am. Chem. Soc.* **2006**, *128*, 14150–14155.

(45) Yu, M. X.; Shi, M.; Chen, Z. G.; Li, F. Y.; Li, X. X.; Gao, Y. H.; Xu, J.; Yang, H.; Zhou, Z. G.; Yi, T.; Huang, C. H. *Chem.—Eur. J.* **2008**, *14*, 6892–6900.

(46) Walt, D. R. *Nat. Mater.* **2002**, *1*, 17–18.

(47) Nolan, E. M.; Lippard, S. J. *J. Mater. Chem.* **2005**, *15*, 2778–2783.

(48) Zhao, Y.; Zhong, Z. Q. *Org. Lett.* **2006**, *8*, 4715–4717.

(49) Sasaki, D. Y.; Padilla, B. E. *Chem. Commun.* **1998**, 1581–1582.

(50) Zhang, X. B.; Guo, C. C.; Li, Z. Z.; Shen, G. L.; Yu, R. Q. *Anal. Chem.* **2002**, *74*, 821–825.

(51) Mancini, F.; Rampazzo, E.; Tecilla, P.; Tonellato, U. *Chem.—Eur. J.* **2006**, *12*, 1844–1854.

(52) Zou, Y.; Yi, T.; Xiao, S. Z.; Li, F. Y.; Li, C. Y.; Gao, X.; Wu, J. C.; Yu, M. X.; Huang, C. H. *J. Am. Chem. Soc.* **2008**, *130*, 15750–15751.

(53) Liu, T.; Hu, J. M.; Yin, J.; Zhang, Y. F.; Li, C. H.; Liu, S. Y. *Chem. Mater.* **2009**, *21*, 3439–3446.

(54) Yin, J.; Guan, X. F.; Wang, D.; Liu, S. Y. *Langmuir* **2009**, DOI: 10.1021/la901377h.

(55) Blanazs, A.; Armes, S. P.; Ryan, A. J. *Macromol. Rapid Commun.* **2009**, *30*, 267–277.

(56) Butun, V.; Billingham, N. C.; Armes, S. P. *J. Am. Chem. Soc.* **1998**, *120*, 11818–11819.

(57) Colfen, H. *Macromol. Rapid Commun.* **2001**, *22*, 219–252.

(58) Alarcon, C. D. H.; Pennadam, S.; Alexander, C. *Chem. Soc. Rev.* **2005**, *34*, 276–285.

(59) Butun, V.; Liu, S.; Weaver, J. V. M.; Bories-Azeau, X.; Cai, Y.; Armes, S. P. *React. Funct. Polym.* **2006**, *66*, 157–165.

(60) Gohy, J. F. *Adv. Polym. Sci.* **2005**, *190*, 65–136.

(61) Liu, S. Y.; Billingham, N. C.; Armes, S. P. *Angew. Chem., Int. Ed.* **2001**, *40*, 2328–2331.

(62) Liu, S. Y.; Armes, S. P. *Angew. Chem., Int. Ed.* **2002**, *41*, 1413–1416.

(63) Shiraishi, Y.; Miyamoto, R.; Zhang, X.; Hirai, T. *Org. Lett.* **2007**, *9*, 3921–3924.

(64) Shiraishi, Y.; Miyamoto, R.; Hirai, T. *Langmuir* **2008**, *24*, 4273–4279.

(65) Uchiyama, S.; Kawai, N.; de Silva, A. P.; Iwai, K. *J. Am. Chem. Soc.* **2004**, *126*, 3032–3033.

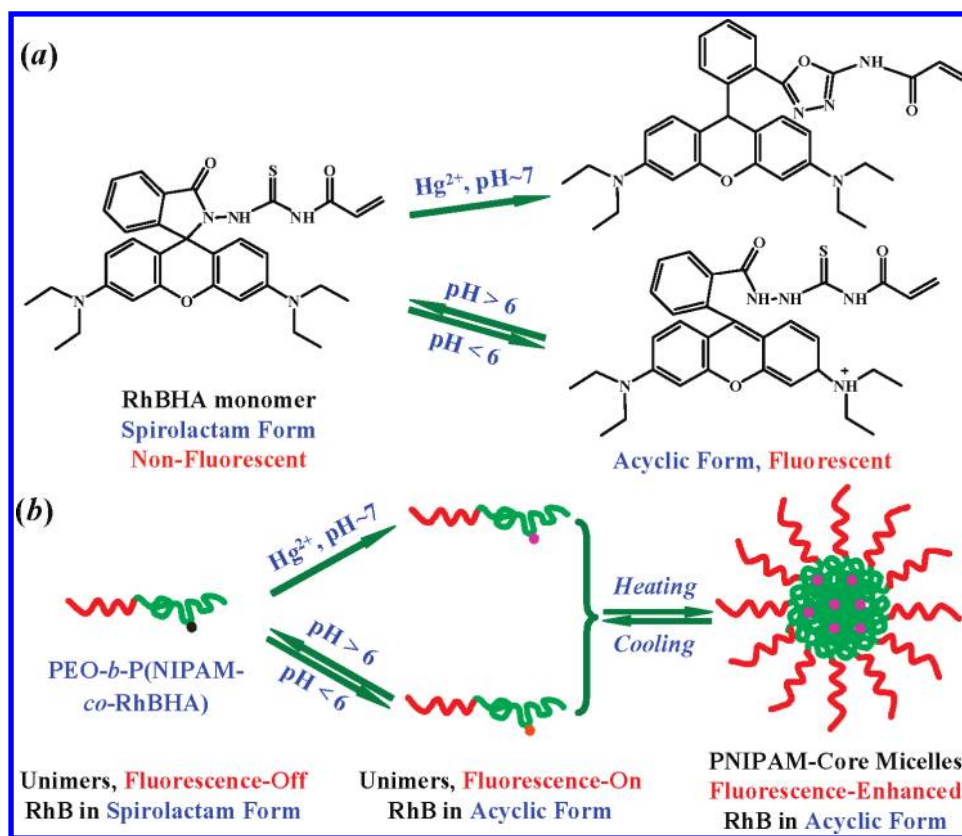
(66) Uchiyama, S.; Matsumura, Y.; de Silva, A. P.; Iwai, K. *Anal. Chem.* **2004**, *76*, 1793–1798.

(67) Iwai, K.; Matsumura, Y.; Uchiyama, S.; de Silva, A. P. *J. Mater. Chem.* **2005**, *15*, 2796–2800.

(68) Skey, J.; O'Reilly, R. K. *Chem. Commun.* **2008**, 4183–4185.

(69) Yang, X. F.; Guo, X. Q.; Zhao, Y. B. *Talanta* **2002**, *57*, 883–890.

Scheme 1. (a) Schematic for the Synthesis of Rhodamine B-Based Spirolactam Monomer (RhBHA) and (b) Proposed Ring-Opened Mechanism in the Presence of Hg^{2+} Ions or Acid Media



(1H, $\text{CH}_2=\text{CH}$), 6.22 (2H, $\text{CH}_2=\text{CH}$). ^{13}C NMR (CDCl_3 , δ , ppm, TMS): 160.6, 147.4, 135.0, 130.9.

Synthesis of RhBHA Monomer (Scheme S2). Rhodamine B hydrazide (0.92 g, 2.0 mmol) was dissolved in 20 mL of dry MeCN. Freshly prepared acryloyl isothiocyanate (0.23 g, 2.0 mmol) in dry MeCN (20 mL) was then added dropwise over 1 h. The reaction mixture was stirred at room temperature for 24 h. The precipitates were collected by filtration and washed with dry MeCN for three times. The crude product was further purified by recrystallization from MeCN for two times. After drying in a vacuum oven overnight at room temperature, RhBHA was obtained as a slightly pink powder (0.83 g, yield: 72%). ^1H NMR (CDCl_3 , δ , ppm, TMS; Figure S1): 11.45 (1H, $-\text{C}(=\text{S})\text{NHCO}-$), 8.74 (1H, $-\text{CON}-\text{NHC}(=\text{S})-$), 8.01 (1H, *ArH*), 7.50 (2H, *ArH*), 7.11 (1H, *ArH*), 6.75 (2H, xanthene-*H*), 6.36 (5H, xanthene-*H*, $-\text{CH}=\text{CHH}$), 6.04 (1H, $-\text{CH}=\text{CHH}$), 5.85 (1H, $-\text{CH}=\text{CHH}$), 3.35 (8H, $-\text{NCH}_2\text{CH}_3$), and 1.17 (12H, $-\text{NCH}_2\text{CH}_3$). ^{13}C NMR (CDCl_3 , δ , ppm, TMS; Figure S1): 181.5 ($-\text{C}=\text{S}$), 168.8, 159.5, 153.8, 151.7, 149.2, 133.4, 132.6, 131.7, 129.6, 128.7, 128.4, 124.1, 123.1, 108.2, 103.8, 98.1, and 66.0 (spiro-C), 44.5, 12.7.

Synthesis of PEO-Based MacroRAFT Agent (Scheme S1). PEO-based macroRAFT agent was prepared by the esterification reaction of PEO $_{113}$ -OH with BTPA in the presence of DCC and DMAP. In a typical procedure, PEO $_{113}$ -OH (10.0 g, 2.0 mmol) was dissolved in anhydrous toluene (25 mL), and then azeotropic distillation was carried out at 50 °C under reduced pressure to remove most of the solvent. BTPA (1.09 g, 4.0 mmol) and dry CH_2Cl_2 (100 mL) were added. After cooling to 0 °C in an ice-water bath, a mixture containing DCC (0.83 g, 4.0 mmol), DMAP (49 mg, 0.4 mmol), and dry CH_2Cl_2 (20 mL) was added dropwise over 1 h. The reaction mixture was stirred at room temperature for 48 h. After removing insoluble salts by filtration, the filtrates were concentrated on a rotary evaporator and then precipitated into an excess of cold diethyl ether. The above dissolution-precipitation cycle was repeated for three times.

After drying in a vacuum oven overnight at room temperature, PEO $_{113}$ macroRAFT agent was obtained as a slightly yellowish powder (9.8 g, yield: 93%). ^1H NMR (CDCl_3 , δ , ppm, TMS; Figure S2): 7.33 (5H, *ArH*), 4.60 (2H, *ArCH}_2-), 4.27 (2H, $-\text{CH}_2\text{OCOCH}_2-$), 3.83–3.58 (452H, $-\text{CH}_2\text{CH}_2\text{O}-$), 3.54 (3H, $\text{CH}_3\text{O}-$), 3.38 (2H, $-\text{CH}_2\text{OCOCH}_2\text{CH}_2\text{SC}(=\text{S})-$), 2.82 (2H, $-\text{CH}_2\text{OCOCH}_2\text{CH}_2\text{SC}(=\text{S})-$).*

Synthesis of PEO-*b*-P(NIPAM-*co*-RhBHA) (Scheme S2). Typical procedures employed for the RAFT synthesis of RhBHA-labeled DHBCs, PEO-*b*-P(NIPAM-*co*-RhBHA), are as follows. Into a reaction tube equipped with a magnetic stirring bar, NIPAM (0.91 g, 8.0 mmol), RhBHA (23 mg, 0.04 mmol), PEO-based macroRAFT agent (0.42 g, 0.08 mmol), AIBN (2 mg, 12 μmol), and 1,4-dioxane (1.4 g) were charged. The tube was carefully degassed by three freeze-pump-thaw cycles and then sealed under vacuum. After thermostating at 70 °C in an oil bath and stirring for 1.5 h, the reaction tube was quenched into liquid nitrogen, opened, and diluted with 1,4-dioxane; the mixture was then precipitated into an excess of diethyl ether. The above dissolution-precipitation cycle was repeated for three times. PEO-*b*-P(NIPAM-*co*-RhBHA) was obtained as a powder with a yield of 63% (0.84 g). GPC analysis revealed an M_n of 14.3 kDa and an M_w/M_n of 1.13 (Figure S3). The degree of polymerization, DP, of P(NIPAM-*co*-RhBHA) was determined to be 69 by ^1H NMR analysis (Figure S2). Thus, the polymer was denoted as PEO $_{113}$ -*b*-P(NIPAM-*co*-RhBHA) $_{69}$. RhBHA content in P(NIPAM-*co*-RhBHA) block was determined to be 0.48 mol % by UV-vis spectroscopy by using RhBHA as the calibration standard in the presence of 5 equiv of Hg^{2+} ions. Following similar procedures, PEO $_{113}$ -*b*-P(NIPAM-*co*-RhBHA) $_{115}$ was also prepared with an M_n of 20.4 kDa and an M_w/M_n of 1.10 (0.46 mol % RhBHA in NIPAM-containing block).

Characterization. Nuclear Magnetic Resonance (NMR) Spectroscopy. All ^1H NMR spectra were recorded on a Bruker AV300 NMR spectrometer (resonance frequency of 300 MHz

for ^1H and 75 MHz for ^{13}C) operated in the Fourier transform mode. CDCl_3 was used as the solvent.

Gel Permeation Chromatography (GPC). Molecular weights and molecular weight distributions were determined by gel permeation chromatography (GPC) equipped with a Waters 1515 pump and a Waters 2414 differential refractive index detector (set at 30 °C). It used a series of two linear Styragel columns (HR2 and HR4) at an oven temperature of 45 °C. The eluent was THF at a flow rate of 1.0 mL/min. A series of low-polydispersity polystyrene standards were employed for calibration.

Laser Light Scattering (LLS). Dynamic and static LLS measurements were conducted on a commercial spectrometer (ALV/DLS/SLS-5022F) equipped with a multitaup digital time correlator (ALV5000) and a cylindrical 22 mW UNIPHASE He–Ne laser ($\lambda_0 = 632 \text{ nm}$) as the light source.

Stopped-Flow Fluorescence. Stopped-flow fluorescence studies were carried out using a Bio-Logic SFM300/S stopped-flow instrument. The SFM-3/S is a three-syringe (10 mL) instrument in which all step-motor-driven syringes (S1, S2, S3) can be operated independently to carry out single- or double-mixing. The SFM-300/S stopped-flow device is attached to the MOS-250 spectrometer. Kinetic data were fitted using the program Biokine (Bio-Logic). For the fluorescence emission detection, the excitation and emission wavelengths (10 nm slit widths in both cases) were set at 500 and 584 nm, respectively. A typical dead time is 2.6 ms using the FC-15 flow cell.

Fluorescence Measurements. Fluorescence spectra were recorded using a RF-5301/PC (Shimadzu) spectrofluorometer. The temperature of the water-jacketed cell holder was controlled by a programmable circulation bath. The slit widths were set at 5 nm for excitation and 3 or 5 nm for emission.

UV–vis Spectroscopy. All UV–vis spectra were acquired on a Unicou UV/vis 2802PCS spectrophotometer. A thermostatically controlled cuvette was employed, and the heating rate was $0.2 \text{ }^\circ\text{C min}^{-1}$.

Results and Discussion

Well-defined DHBCs bearing rhodamine B-based Hg^{2+} -sensing moieties in the thermo-responsive block were synthesized via reversible addition–fragmentation chain transfer (RAFT) polymerization using PEO-based macroRAFT agent (Scheme S1 in the Supporting Information). Novel polymerizable Hg^{2+} -sensing monomer, RhBHA, was prepared at first. The rhodamine urea derivative was nonfluorescent in the spirolactam form and can be selectively converted into the fluorescent ring-opened amide form in the presence of Hg^{2+} ions or in acidic media (Scheme 1a).^{2,43–45,63} The content of sensing moieties, RhBHA monomer, in the P(NIPAM-co-RhBHA) block was determined to be $\sim 0.5 \text{ mol } \%$. The thermo-induced aggregation of the DHBCs was investigated by temperature-dependent optical transmittance, laser light scattering (LLS). Temperature-dependent transmittance measurements revealed that $\text{PEO}_{113}\text{-}b\text{-P(NIPAM-co-RhBHA)}_{69}$ and $\text{PEO}_{113}\text{-}b\text{-P(NIPAM-co-RhBHA)}_{115}$ DHBCs undergo thermo-induced aggregation above ~ 36 and $34 \text{ }^\circ\text{C}$, respectively, due to the lower critical solution temperature (LCST) phase behavior of NIPAM-containing blocks (Figure S4). Moreover, these DHBCs exhibit an amphiphilic character at around body temperatures, providing extra advantages for their in vivo applications.^{70–74} As revealed by dynamic laser light scattering (LLS), $\text{PEO}_{113}\text{-}b\text{-P(NIPAM-co-RhBHA)}_{69}$

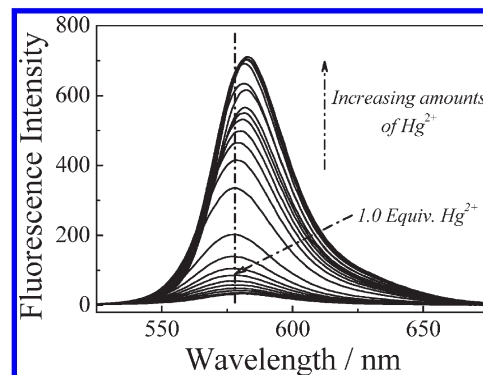


Figure 1. Fluorescence spectra recorded for 0.05 g/L aqueous solution of $\text{PEO}_{113}\text{-}b\text{-P(NIPAM-co-RhBHA)}_{69}$ at pH 7 and 25 °C ($\lambda_{\text{ex}} = 500 \text{ nm}$; slit widths: Ex 5 nm, Em 5 nm; [RhBHA] = 1.25 μM) upon gradual addition of Hg^{2+} (0–5 equiv relative to RhBHA residues).

molecularly dissolves as unimers in water at 25 °C with an intensity-average hydrodynamic radius, $\langle R_h \rangle$, of 3.4 nm and self-assembles at 40 °C into P(NIPAM-co-RhBHA)-core aggregates with $\langle R_h \rangle$ of 80.6 nm and size polydispersity of 0.053 (Figure S5). Static LLS revealed an average aggregation number of 4.9×10^3 (Figure S6). Thus, there exist ~ 1600 RhBHA sensing moieties per micelle.

PEO-*b*-P(NIPAM-co-RhBHA) DHBCs as Multifunctional Sensors. We then investigated the Hg^{2+} -sensing capability of $\text{PEO-}b\text{-P(NIPAM-co-RhBHA)}$ DHBCs in their unimer state at 25 °C. Typical fluorescence emission and absorbance spectra obtained for aqueous solution of $\text{PEO}_{113}\text{-}b\text{-P(NIPAM-co-RhBHA)}_{69}$ (0.05 g/L, [RhBHA] = 1.25 μM) upon gradual addition of Hg^{2+} ions are shown in Figure 1 as well as Figures S7 and S8. Fluorescence intensity dramatically increases upon ions addition and stabilizes above ~ 4 equiv of Hg^{2+} ions (relative to RhBHA residues), exhibiting a 22-fold cumulative enhancement. Concomitantly, we can discern a slight red shift of the maximum emission peak from 578 to 584 nm in the same range of $[\text{Hg}^{2+}]$. Absorbance spectra also exhibit a clear increase at $\sim 565 \text{ nm}$. Simple visual inspection revealed a colorless to pink transition under visible light and a colorless to orange transition under UV 365 nm upon Hg^{2+} addition (Figure S9). Moreover, among a series of cations including K^+ , Na^+ , Li^+ , Co^{2+} , Cd^{2+} , Pb^{2+} , Zn^{2+} , Fe^{2+} , Fe^{3+} , Ca^{2+} , Ag^+ , Cu^{2+} , and Hg^{2+} (5 equiv), only Hg^{2+} exhibits the apparent fluorescence enhancement (colorless to orange transition) within 10 min upon addition (Figure S9). This indicates that the incorporation of rhodamine urea moieties into DHBCs does not alter their selective Hg^{2+} -sensing capability.

The selectivity of $\text{PEO}_{113}\text{-}b\text{-P(NIPAM-co-RhBHA)}_{69}$ to the detection of Hg^{2+} ions were further investigated by fluorescence and absorbance measurements. Upon long standing (5 h) after the addition of various cations, Ag^+ ions can induce a 3-fold increase of fluorescence intensity at 584 nm (Figure 2, Figure S10). Time-dependent fluorescence studies reveal that the fluorescence intensity increase induced by Ag^+ ions actually occurs 40 min after addition (Figure S11), and this is in agreement with that reported by other research groups for small molecule rhodamine urea derivatives.³⁶ Employing the stopped-flow technique, we observed that the Hg^{2+} -induced fluorescence “turn-on” process is completed within 2–3 ms (Figure S12), which is much shorter than that of Ag^+ ions. From Figure S9, we can visually observe that Cu^{2+} ions addition can induce a colorless to purple transition, whereas no fluorescence enhancement can be discerned

(70) Schild, H. G. *Prog. Polym. Sci.* **1992**, *17*, 163–249.

(71) Yan, J. J.; Ji, W. X.; Chen, E. Q.; Li, Z. C.; Liang, D. H. *Macromolecules* **2008**, *41*, 4908–4913.

(72) Okada, Y.; Tanaka, F. *Macromolecules* **2005**, *38*, 4465–4471.

(73) Zhang, W. Q.; Shi, L. Q.; Wu, K.; An, Y. G. *Macromolecules* **2005**, *38*, 5743–5747.

(74) Ono, Y.; Shikata, T. *J. Am. Chem. Soc.* **2006**, *128*, 10030–10031.

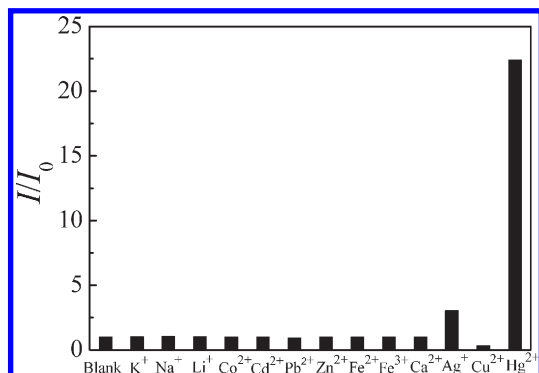


Figure 2. Variation of relative fluorescence intensity (584 nm) of 0.05 g/L aqueous solution of PEO₁₁₃-*b*-P(NIPAM-*co*-RhBHA)₆₉ (pH 7, 25 °C) within 5 h after the addition of 5 equiv of K⁺, Na⁺, Li⁺, Co²⁺, Cd²⁺, Pb²⁺, Zn²⁺, Fe²⁺, Fe³⁺, Ca²⁺, Ag⁺, Cu²⁺, and Hg²⁺.

under UV light (Figure 2, Figures S9 and S10). Further absorbance studies indicate that Cu²⁺ ions can induce a nearly quantitative titration of RhBHA residues, as observed by the almost linear increase of absorbance intensity (564 nm) up to [Cu²⁺]/[RhBHA] = 1.2 (Figure S13). Interestingly, Cu²⁺ ions tend to completely quench the fluorescence of RhBHA moieties in their acyclic form (Scheme 1b, Figure 2, Figures S9 and S10). On the basis of the above results, we conclude that PEO-*b*-P(NIPAM-*co*-RhBHA) DHBCs in the unimers state can serve as highly selective and sensitive fluorescent/colorimetric chemosensors to Hg²⁺ ions. Most importantly, qualitative differentiation between Hg²⁺, Cu²⁺, Ag⁺ ions, and other competitive cations can be accomplished just by simple visual inspections.

Within thermo-induced aggregates of PEO-*b*-P(NIPAM-*co*-RhBHA) diblock copolymer in aqueous solution, Hg²⁺-induced ring-opened amide form of RhBHA residues are located within hydrophobic cores, and this will enhance the fluorescence quantum yield of fluorescent reporters and achieve a signal amplification effect.^{2,43–45,63} Fluorescence emission spectra obtained for the aqueous solution of PEO₁₁₃-*b*-P(NIPAM-*co*-RhBHA)₆₉ upon addition of 5 equiv of Hg²⁺ in the temperature range of 20–45 °C are shown in Figure S14. It was found that upon addition of Hg²⁺ ions at 40 °C the fluorescence intensity exhibits a further 3.5-fold increase, as compared to that at 25 °C. The fluorescence enhancement was only observed at temperatures above 36 °C, which is in agreement with the critical micellization temperature obtained by temperature-dependent optical transmittance (Figure S4). If we define the detection limit as the Hg²⁺ ions concentration at which a 10% fluorescence enhancement can be measured by employing 0.01 g/L aqueous solution of PEO₁₁₃-*b*-P(NIPAM-*co*-RhBHA)₆₉, the Hg²⁺ ions detection limit considerably improves from 3.5 to 1.6 ppb upon the temperature increase from 25 to 40 °C (Figure 3). The above results indicate that the incorporation of selective Hg²⁺-sensing rhodamine urea residues into the thermo-responsive block of PEO-*b*-P(NIPAM-*co*-RhBHA) DHBCs can obviously enhance the detection sensitivity via thermo-induced self-organization, and an overall 77-fold fluorescence “turn-on” has been achieved; an obvious fluorescence emission intensity enhancement is shown in Figure 4.

Considering that nonfluorescent rhodamine urea moieties also undergo reversible transformation into fluorescent ring-opened amide form in acidic media (Scheme 1a),⁶³ we also attempted employing PEO-*b*-P(NIPAM-*co*-RhBHA) DHBCs as pH sensors. Above pH 6, the aqueous solution of PEO₁₁₃-*b*-P(NIPAM-*co*-RhBHA)₆₉ remains colorless and essentially nonfluorescent at

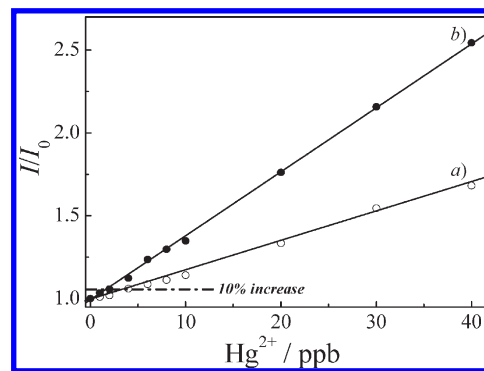


Figure 3. Variation of relative fluorescence intensity (584 nm) of 0.01 g/L aqueous solution of PEO₁₁₃-*b*-P(NIPAM-*co*-RhBHA)₆₉ (pH 7; λ_{ex} = 500 nm, slit widths: Ex 5 nm, Em 5 nm; [RhBHA] = 0.25 μM) recorded at (a) 25 °C and (b) 40 °C upon gradual addition of Hg²⁺ (0–40 ppb).

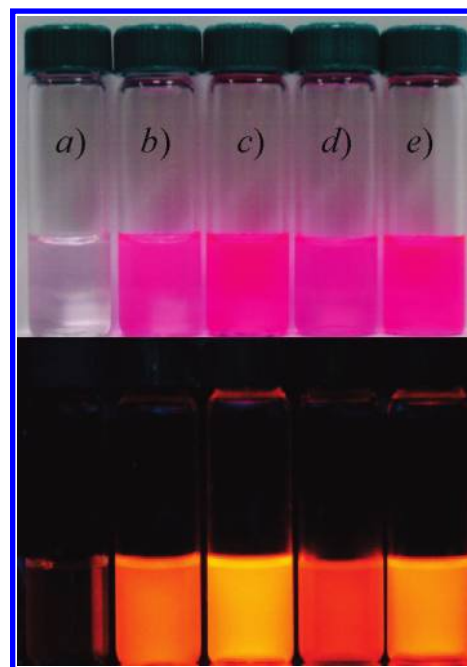


Figure 4. Photographs recorded under visible light (top) and UV 365 nm (bottom) for aqueous solutions of PEO₁₁₃-*b*-P(NIPAM-*co*-RhBHA)₆₉ at different solution conditions: (a) pH 7, 25 °C, no Hg²⁺; (b) pH 7, 25 °C, 5 equiv of Hg²⁺; (c) pH 7, 40 °C, 5 equiv of Hg²⁺; (d) pH 3, 25 °C, no Hg²⁺; (e) pH 3, 40 °C, no Hg²⁺.

25 °C, which indicates that RhBHA residues are in the spiro-lactam form. However, in the range of pH 1–6 at 25 °C, a colorless to pink transition under visible light and a colorless to orange transition under UV 365 nm irradiation also can be visualized by the naked eye (Figure 4), just similar to those observed for Hg²⁺-induced visual changes at pH 7 (Figure 4, Figure S9). This has been further confirmed by pH-dependent absorbance and fluorescence studies (Figure 5, Figure S15). Accompanied by the dramatic increase of absorbance intensity at 565 nm in the range of pH 1–6 at 25 °C, fluorescence intensity also exhibits a 25-fold increase (Figures 5 and 6).

For RhBHA residues in PEO-*b*-P(NIPAM-*co*-RhBHA) DHBCs, the fully reversible nature of pH-induced switching between nonfluorescent spiro-lactam and highly fluorescent acyclic forms has been verified by fluorescence measurements upon pH cycles between 3 and 7 (Figure 7). Moreover, we observed that the pH detection sensitivity can also be enhanced

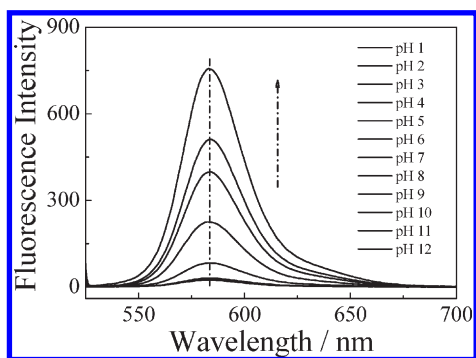


Figure 5. Fluorescence emission spectra ($\lambda_{\text{ex}} = 500$ nm, slit widths: Ex 5 nm, Em 5 nm) recorded for 0.05 g/L aqueous solution (25 °C) of $\text{PEO}_{113}\text{-}b\text{-P}(\text{NIPAM}\text{-}co\text{-RhBHA})_{69}$ in the pH range of 1–12.

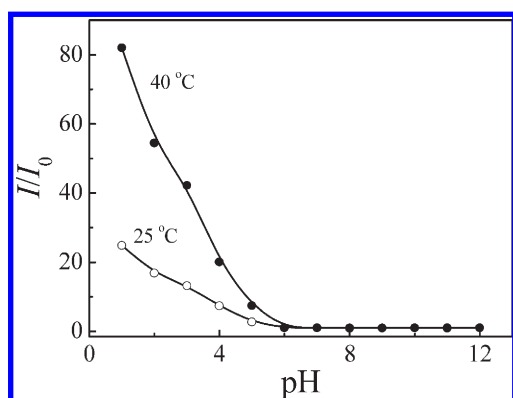


Figure 6. pH-dependent relative fluorescence intensity ($\lambda_{\text{ex}} = 500$ nm, $\lambda_{\text{em}} = 584$ nm) recorded for 0.05 g/L aqueous solution at 25 and 40 °C.

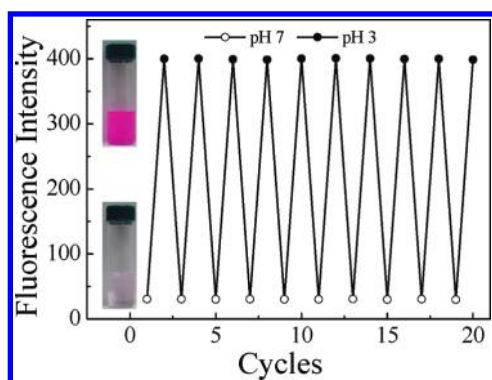


Figure 7. Change in fluorescence emission intensity of 0.05 g/L aqueous solution of $\text{PEO}_{113}\text{-}b\text{-P}(\text{NIPAM}\text{-}co\text{-RhBHA})_{69}$ at 25 °C when solution pH was cycled between 3 and 7.

by the thermo-induced aggregation of $\text{PEO}\text{-}b\text{-P}(\text{NIPAM}\text{-}co\text{-RhBHA})$, as revealed by visual inspection of the dispersion at 25 and 40 °C for a fixed pH of 3 (Figure 4). At 40 °C, fluorescence intensity at 584 nm exhibits a 82-fold increase in the pH range of 1–6 (Figure 6). The more dramatic pH-induced

changes of relative fluorescence intensity at 40 °C compared to that at 25 °C imply an enhancement of detection sensitivity in the range of pH 1–6, which is quite reasonable considering that fluorescent ring-opened RhBHA residues are located in a non-polar environment at elevated temperatures, i.e., hydrophobic cores of thermo-induced aggregates.^{2,43–45,63}

Actually, the positive effect on the pH detection sensitivity exerted by temperatures also suggests that $\text{PEO}\text{-}b\text{-P}(\text{NIPAM}\text{-}co\text{-RhBHA})$ DHBCs can serve as excellent digital thermometers with tunable sensitivity (Figure S16). At pH 7, we cannot discern any appreciable fluorescence intensity changes in the temperature range of 20–45 °C, which is reasonable considering that RhBHA residues remain in the nonfluorescent spirolactam form. However, at pH 5 and 3, we are able to achieve a 2.6-fold and a 3.3-fold increase in fluorescence intensity, respectively, in the same temperature range. Thermo-induced colorimetric and fluorescent changes can also be facily checked by the naked eye, as depicted in Figure 4. It should be noted that the detectable temperature range of $\text{PEO}\text{-}b\text{-P}(\text{NIPAM}\text{-}co\text{-RhBHA})$ DHBCs can be facily adjusted by the DP of $\text{P}(\text{NIPAM}\text{-}co\text{-RhBHA})$ block. As shown in Figure S4, $\text{PEO}_{113}\text{-}b\text{-P}(\text{NIPAM}\text{-}co\text{-RhBHA})_{69}$ and $\text{PEO}_{113}\text{-}b\text{-P}(\text{NIPAM}\text{-}co\text{-RhBHA})_{115}$ DHBCs possess LCSTs of ~ 36 and 34 °C, respectively.

Conclusion

In summary, double hydrophilic block copolymers bearing RhB-based Hg^{2+} -reactive moieties in the thermo-responsive block were synthesized, which can serve as multifunctional sensors to pH, temperature, and Hg^{2+} ions. Moreover, the detection sensitivity to pH and Hg^{2+} ions can be considerably enhanced at elevated temperatures via the formation of hydrophobic domains within thermo-induced micellar aggregates of DHBCs. This work represents the first example of responsive DHBC-based multifunctional chemosensors for the highly efficient detection of Hg^{2+} ions, pH, and temperatures. The combination of stimuli-responsive block copolymers with well-developed small molecule-based selective sensing moieties in the current study are expected to exhibit preferred advantages including enhanced detection sensitivity, water dispersibility, biocompatibility, facily integration into devices, and the ability of further functionalization for targeted delivery and imaging. Further works toward this aspect, including the fabrication of stimuli-responsive block copolymer-based ratiometric FRET sensors, are currently underway.

Acknowledgment. The financial support of the National Natural Scientific Foundation of China (NNSFC) Projects (20534020, 20674079, and 20874092) and Specialized Research Fund for the Doctoral Program of Higher Education (SRFDP) is gratefully acknowledged.

Supporting Information Available: ^1H and ^{13}C NMR, GPC, dynamic and static LLS, UV–vis, and fluorescence characterization results. This material is available free of charge via the Internet at <http://pubs.acs.org>.